

Supporting information for:

Hypericin: Single Molecule Spectroscopy of an Active Natural Drug

Quan Liu,^{[a][c]} Frank Wackenhet,^{[a]} Otto Hauler,^{[a][b]} Miriam Scholz,^{[a][b]} Sven zur Oven-Krockhaus,^{[a][d]} Rainer Ritz,^[e] Pierre-Michel Adam,^[c] Marc Brecht^{[a][b]} and Alfred J. Meixner^{[a]*}*

[a] Institute of Physical and Theoretical Chemistry, Eberhard Karls University Tübingen,
Auf der Morgenstelle 18, 72076 Tübingen, Germany

[b] Reutlingen Research Institute, Process Analysis and Technology (PA&T), Reutlingen
University, Alteburgstraße 150, 72762 Reutlingen, Germany

[c] Laboratoire Lumière, nanomatériaux & nanotechnologies – L2n, Université de
Technologie de Troyes & CNRS ERL 7004, 12 rue Marie Curie, 10000 Troyes, France

[d] Center for Plant Molecular Biology (ZMBP), Eberhard Karls University Tübingen, Auf
der Morgenstelle 32, 72076 Tübingen, Germany

[e] Department of Neurosurgery, Schwarzwald-Baar Clinic, Klinikstraße 11, 78052 Villingen-Schwenningen, Germany

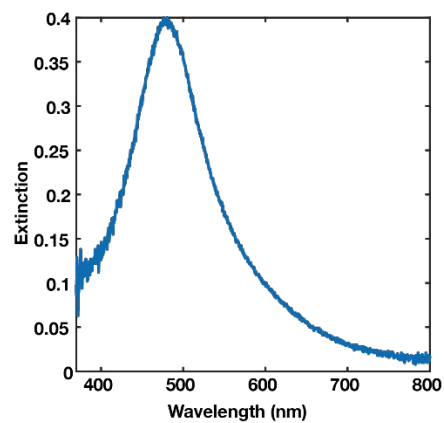


Figure S1. Extinction spectrum of the SERS substrate with a particle plasmon band at 482 nm.

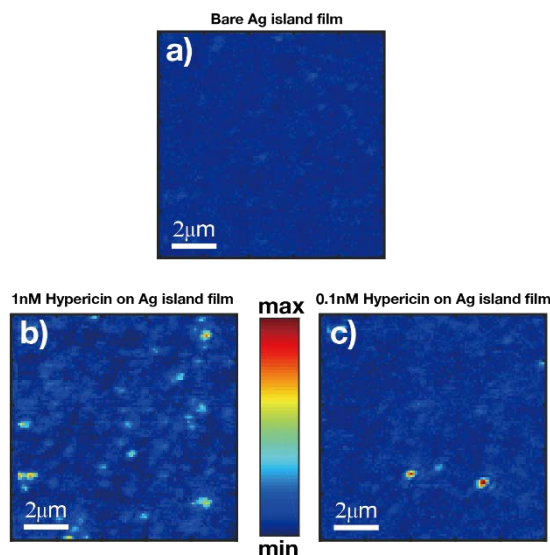


Figure S2. SERS scanning image. (a) shows scanning image of an Ag island film before deposition of hypericin; (b,c) show SERS signal images after drop-casting of 10^{-9} M and 10^{-10} M Hypericin on Ag island film, respectively. After deposition of hypericin diffraction limited and intense hot spots can be observed, which are used to acquire the single molecule SERS spectra shown in Figure 5 (c) and (d). The excitation laser was 530nm (0.4 μ W), scanning range was 10 μ mX10 μ m for all images.

Table S1. SERS peak positions in cm^{-1} and relative intensities (in brackets) are given for the ensemble spectrum shown in Fig. 5(b), the deprotonated (Hyp^-) and neutral (Hyp) SM shown in Fig. 5(c) and the respective simulated spectra.

Ensemble	Exp. Hyp ⁻	Sim. Hyp ⁻	Exp. Hyp	Sim. Hyp	assignment ⁸
309 (0.04)		319 (0.28)		321 (0.09)	
358 (0.04)		342 (0.35)		349 (0.20)	
450 (0.35)	448 (0.19)	438 (0.39)	455 (0.19)	459 (1.00)	Skeletal deformation
476 (0.17)		465 (0.37)		490 (0.13)	Skeletal deformation
	529 (0.18)	518 (0.11)	518 (0.10)	510 (0.13)	Skeletal deformation
			593 (0.08)	600 (0.08)	Skeletal deformation
630 (0.13)	636 (0.32)	639 (0.12)	637 (0.15)	636 (0.05)	
665 (0.09)		667 (0.08)	746 (0.09)		
699 (0.07)		682 (0.08)		700 (0.04)	
763 (0.11)					
816 (0.07)	830 (0.47)	808 (0.04)	790 (0.14)	814 (0.02)	
862 (0.07)	868 (0.56)	848 (0.08)	839 (0.14)	850 (0.09)	
933 (0.12)	938 (0.13)	918 (0.17)	939 (0.13)	936 (0.17)	
1018 (0.03)	1017 (0.10)	1017 (0.02)	1016 (0.12)	1025 (0.02)	
1134 (0.09)	1129 (0.67)	1122 (0.17)	1125 (0.44)	1119 (0.16)	C-H bending
1189 (0.13)	1168 (0.56)	1177 (0.16)		1190 (0.12)	C-O stretching
1251 (0.44)	1232 (0.70)	1223 (0.24)	1230 (0.63)	1225 (0.24)	Ring in plane
1297 (1.00)	1299 (1.00)	1298 (1.00)		1298 (0.46)	Ring in plane
1333 (0.77)	1364 (0.82)	1324 (0.69)	1316 (0.76)	1327 (0.97)	Ring in plane
1380 (0.66)	1405 (0.46)	1380 (0.26)	1398 (0.92)	1395 (0.22)	Ring in plane
1450 (0.24)	1471 (0.33)	1467 (0.20)	1451 (0.39)	1444 (0.20)	Ring in plane
1514 (0.19)	1525 (0.24)	1514 (0.17)	1480 (0.28)	1514 (0.40)	

1589 (0.87)	1564 (0.21)	1545 (0.57)	1571 (0.58)	Ring stretching with C=O
1604 (0.30)	1613 (0.49)	1614 (0.07)	1610 (1.00)	C=O stretching
1648 (0.29)		1625 (0.07)		1633 (0.13)